Scripta Materialia 149 (2018) 21–25

Contents lists available at ScienceDirect

Scripta Materialia

journal homepage: www.elsevier.com/locate/scriptamat

Regular article

Structural relaxation kinetics defines embrittlement in metallic glasses

Jittisa Ketkaew [a], Meng Fan [a], Mark D. Shattuck [a,b], Corey S. O'Hern [a,c,d], Jan Schroers [a,*]

[a] Department of Mechanical Engineering & Materials Science, Yale University, New Haven, CT 06511, USA
[b] Department of Physics and Benjamin Levich Institute, City College of the City University of New York, New York 10031, USA
[c] Department of Physics, Yale University, New Haven, CT 06511, USA
[d] Department of Applied Physics, Yale University, New Haven, CT 06520, USA

ARTICLE INFO

Article history:
Received 5 December 2017
Received in revised form 22 January 2018
Accepted 23 January 2018
Available online xxxx

Keywords:
Bulk metallic glass
Fracture toughness
Aging
Annealing
Relaxation kinetics

ABSTRACT

Structural relaxation during isothermal annealing, quantified by enthalpy recovery of $Zr_{44}Ti_{11}Cu_{10}Ni_{10}Be_{25}$ towards its metastable equilibrium and correlation to embrittlement, quantified through fracture toughness, K_Q, is studied. Enthalpy relaxation over time obeys the Kohlrausch-William-Watts (KWW) stretch exponent with $\beta = 0.74$ and $\tau = 11{,}000$ s. Such β and τ are used to fit experimental $K_Q(t)$ with KWW, resulting in $R^2 = 0.79$. This finding combined with a controlled characterization of the glasses' K_Q versus temperature, fictive temperature, and their combination, revealed that embrittlement in metallic glasses is predominantly controlled by structural rearrangements, whereas volume changes from thermal expansion have negligible influence.

Structural relaxation, the evolution of a glass towards its metastable equilibrium of the supercooled liquid state is one of the most widely studied and richest topics in glasses. The kinetics and characteristics of structural relaxation are often described by the stretch exponent function, the Kohlrausch-William-Watts [1,2] (KWW) exponent which takes into account the plurality of relaxation processes that typically occurs simultaneously.

As structural relaxation reflects how the structure of a glass evolves towards the (metastable) equilibrium structure of the supercooled liquid, it reveals information about the structure, kinetics, and, when correlated with properties, generally reveals processing-structure-property relationships [3]. Due to the complexity of polymer or molecular glasses, relaxation characteristics in these glasses have been widely observed to obey KWW behavior [4–8]. For the seemingly "simple" metallic glasses (MG's) it is even more surprising that they also follow a KWW relaxation characteristics for their structure [9–12] and related properties such as free volume [13,14], density [15], and viscosity [16].

Annealing induced relaxation of a glass towards the supercooled liquid state in MGs has also been associated with the degradation of mechanical properties, so-called embrittlement, quantified in bending ductility [17–22], tension and compression plasticity [23,24], impact toughness [25,26], and fracture toughness [27–29]. Although previous investigations suggested a correlation between mechanical properties and relaxation process conceptualized as free volume [30,31], the specific correlation between the evolution and kinetics of relaxation and embrittlement were left inconclusive [27,32–35]. For example, it was inconclusive if the reduction of the free volume has been responsible for the embrittlement, and/or what contribution of annealing induced crystallization plays a role [36]. Even though free volume has been suggested widely as a key player in annealing induced embrittlement, previous discussions do not go past a general reduction in density as a free volume change. Isothermal relaxation kinetics of a glass towards its corresponding supercooled liquid, measured by enthalpy changes, has been identified to originate from structural rearrangements processes and not the thermal expansion contribution to the free volume [3,37–41]. Hence, identifying the correlation between enthalpy relaxation and embrittlement kinetics would constitute a powerful step to reveal the mechanism of embrittlement and beyond, fracture toughness in MG's in general.

One of the most direct measurements of embrittlement is fracture toughness measurements. However, until recently such measurements have been difficult and often overshadowed by extrinsic and possible intrinsic effects [42,43]. Since the main objective of this study is to understand how structural relaxation kinetics affect the MG's mechanical behavior, precise measurements are needed to reveal even small changes. We have developed a method that allows precise measurement of the conditional (notched) fracture toughness, K_Q, within 3% sample-to-sample variation once MGs undergo identical processing condition [44], and shown that K_{IC} can be extrapolated from K_Q [45]. This method has enabled to reveal complex processing-property relationships and extrinsic effects on K_Q [46–50].

We apply such method to study the K_Q of the glass and supercool liquid with i). the characterization temperature (T), ii). the fictive

* Corresponding author.
E-mail address: jan.schroers@yale.edu (J. Schroers).

https://doi.org/10.1016/j.scriptamat.2018.01.024
1359-6462/

temperature (T_f), and iii). the relaxation kinetics of the glass towards the supercooled (equilibrium) liquid as a function of time. The fictive temperature, T_f, of a glass is the temperature where the glass had the same enthalpy with the liquid, which can also be viewed as the temperature where the glass falls out of the equilibrium (Fig. 1(c)). As the absolute temperature of the glass is changed, enthalpy of the glass changes due to thermal contraction which is an affine expansion of the glass. On the fictive temperature scale, the structure of the glass changes in a non-affine manner. As a consequence, the response of a glass to temperature variations involves only thermal contraction. This is in contrast to a glass's responses to changes in T_f (characterized at the same T) where only structural changes occur. These two contributions can be quantified from experimental results on thermal expansion of BMG alloys in their glass state and supercooled liquid state. The overall free volume contributes of both terms, which are approximately comparable in their magnitude [51]. We probe such changes through K_Q and enthalpy measurements. We revealed that embrittlement quantified by K_Q measurements follows the same KWW kinetics to enthalpy relaxation kinetics.Comparison between $K_Q(T_f)$ and $K_Q(T)$ reveals that annealing induced embrittlement is controlled predominantly by the structural rearrangement contribution of the free volume. Volumetric thermal contractions contribution occurring on the temperature scale have a negligible effect on K_Q. This implies that overall enthalpy (free volume), which comprises of both, the structural rearrangement and thermal expansion counterparts, is insufficient to quantify the fracture toughness of a glass.

$Zr_{44}Ti_{11}Ni_{10}Cu_{10}Be_{25}$ was used to study the relationship between enthalpy relaxation and K_Q upon isothermal annealing. To understand the effect of structural relaxation on K_Q, appropriate relaxation timescales were estimated using the Vogel-Fulcher-Tammann (VFT) relation, $\tau = \tau_0 \exp(\frac{D^* T}{T - T_0})$, where D^* is the fragility parameter, T_0 is the temperature at which $\tau \to \infty$, and τ_0 the relaxation time in the limit as $1/T \to 0$ and is estimated to be ~2.5×10^{-13} s for Zr-BMG systems [52]. D^* and T_0 are fitting parameters which are obtained by calorimetry as explained elsewhere [32]. We estimated D^* to be 28 and T_0 to be 344 K, giving τ of approximately 20,000 s. To study the relaxation time-dependent K_Q response towards metastable equilibrium, we selected various annealing times including $t = 0, 0.1\tau, 0.5\tau, 1\tau, 2\tau, 4\tau$ at a constant temperature below the calorimetry glass transition temperature, T_g.

Single edge notched tension (SENT) samples with geometry of 25 × 5 × 0.3 mm (length x width x thickness) with precisely controlled notch root radius $\rho = 10$ μm and notch length of 2.5 mm ($a/W = 0.5$) were prepared as described in Fig. 1(a)–(b). As previously shown that the considered MG exhibit a flaw tolerance behavior, the considered notch radius is below the critical notch radius, hence result in approximately the same K_Q as for the sample with an infinitely sharp notch radius [53]. MGs were thermoplastically formed into the as-prepared mold under pressure of 20 MPa at 698 K ($T_g = 623$ K), for 100 s, followed by rapid quenching. This procedure results in uniform and fully amorphous test samples. Samples were then subjected to sub-T_g annealing, which was chosen to avoid decomposition and crystallization, in a temperature-calibrated salt bath system at 593 K for various times (Fig. 1(c) path 3), followed by rapid quenching to prevent further relaxation upon cooling. To reveal the importance of free volume contributions due to thermal contraction, we characterized glasses at different temperatures (Fig. 1(c) path 2) and glasses with different T_f's, which was characterized at the room temperature (superimposed by the change in T). Enthalpy relaxation (ΔH_{rel}) due to annealing was quantified by Differential Scanning Calorimetry (Perkin Elmer Diamond DSC) upon heating with 20 K/min. K_Q tests were conducted by uniaxial tension under a quasi-static displacement controlled mode with a strain rate of 10^{-4} s^{-1} by Instron 5543. Qimaging CCD camera was utilized to observe in-situ plastic zone development during experiment (Fig. 1(d)).

Structural relaxation of $Zr_{44}Ti_{11}Ni_{10}Cu_{10}Be_{25}$ quantified by ΔH_{rel} for various relaxation times is shown in Fig. 2. Relaxation follows a

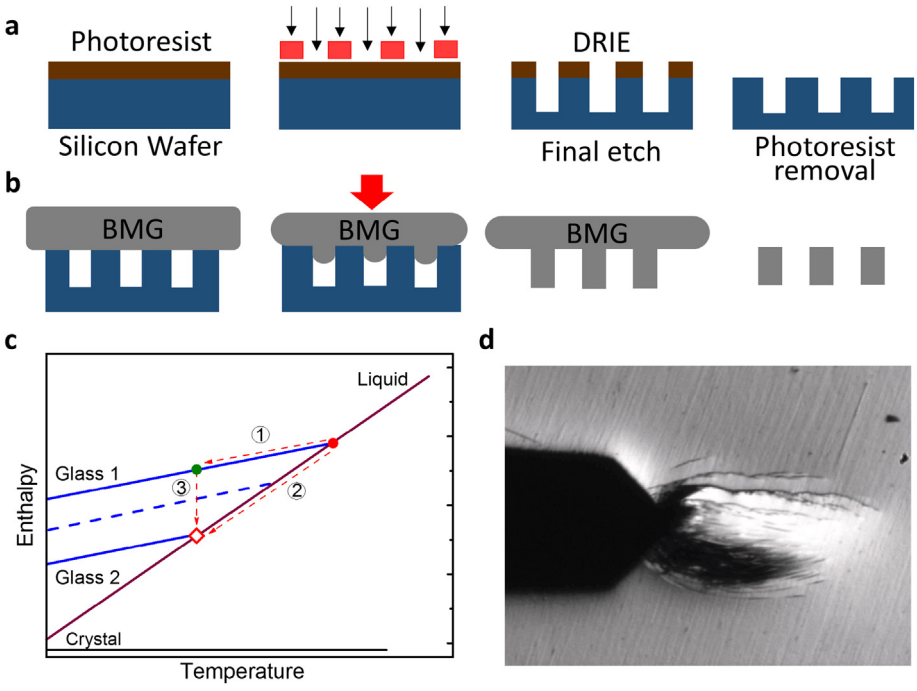

Fig. 1. Single edge notched tension (SENT) specimen fabrication method. (a) Silicon molds were prepared by a photolithography and deep reaction ion etching technique. (b) Thermoplastic forming of $Zr_{44}Ti_{11}Cu_{10}Ni_{10}Be_{25}$ MG into as-prepared silicon mold by compression under a temperature above the material's T_g. Samples were released from the silicon molds by 20% KOH etchant, followed by sanding and polishing procedure. (c) Possible paths for enthalpy changes, Path 1:liquid taken out of equilibrium to form a glass by cooling faster than the internal relaxation rate to maintain equilibrium which results in thermal contraction. Path 2: Cooling is carried out such that the liquid remains in metastable equilibrium. The liquid undergoes rearrangements and thermal contraction. Path 3, a glass is isothermally annealed to allow structural relaxation from its unstable glass state to the metastable equilibrium liquid state. (d) shows typical plastic zone region of $Zr_{44}Ti_{11}Cu_{10}Ni_{10}Be_2$ SENT sample before fracture.

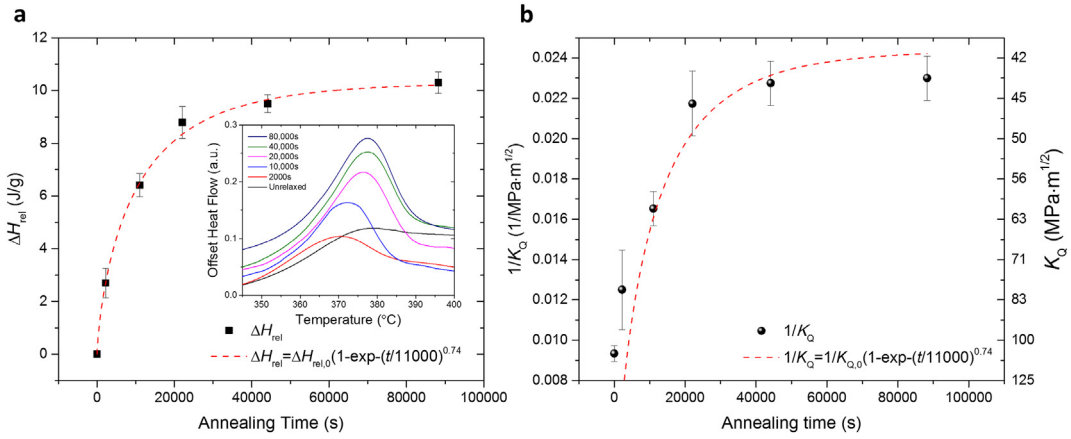

Fig. 2. (a) Recovered enthalpy, ΔH_{rel} versus annealing time for $Zr_{44}Ti_{11}Ni_{10}Cu_{10}Be_{25}$ metallic glasses relaxed at 593 K. Dash line corresponds to fitting curve according to Eq. (1). The inset displays the enthalpy relaxation event. (b) Inverted fracture toughness ($1/K_Q$) versus annealing time. Dash line represents KWW fit of Eq. (3). Fitting parameters as determined by enthalpy recovery experiment were used. K_Q of unrelaxed glass was not considered in the fitting since it does not yet exhibit any characteristic or structure to the isothermal annealing temperature considered here.

stretched exponential behavior, fitted by

$$\Delta H_{rel} = \Delta H_{rel,0}\left[1 - \exp - \left(\frac{t}{\tau_{KWW}}\right)^{\beta}\right] \quad (1)$$

where $\Delta H_{rel,0}$ is the enthalpy of the fully relaxed sample at 593 K, t is the annealing time, τ_{KWW} is the average relaxation time and β is the Kohlrausch exponent. A value of $\beta = 1$ indicates the presence of a single relaxation mechanism. $\beta < 1$ reflects multiple relaxation mechanisms occurring simultaneously, hence broader distribution of relaxation times [5,6,54]. Fitting of the experimental data was carried out following χ^2 minimization algorithm. The quality of the fitting of Eq.(1) to the experimental enthalpy relaxation of $R^2 = 0.99$ reveals a KWW behavior with $\beta = 0.74$, $\tau_{KWW} = 11{,}000$ s, and $\Delta H_{rel,0} = 10.3$ J/g.

Alternatively, β can also be calculated using Eq.(2) [55],

$$\beta = 1 - \sqrt{\frac{T_0/T_g}{D^*}} \quad (2)$$

Calculated β from Eq.(2) gives $\beta = 0.89$, comparable but slightly higher than $\beta = 0.74$ from KWW fitting determined by ΔH_{rel} measurement. This is reasonable as Eq. (2) estimates β as the system approaches T_g of approximately 623 K. It has been experimentally observed that β decreases with decreasing temperature [14,16,56–58]. Parameters determined here also compare well with previously reported values of the same alloy at similar annealing temperatures (595 K) of $\beta = 0.76$ [59].

K_Q measurements were carried out at room temperature (RT) for samples isothermally relaxed at various times that are identical to the enthalpy recovery experiments (Fig. 2(a)). To quantify embrittlement and compare with the kinetics of enthalpy we consider $1/K_Q$ instead:

$$1/K_Q = 1/K_{Q,0}\left[1 - \exp - \left(\frac{t}{\tau_{KWW}}\right)^{\beta}\right] \quad (3)$$

Dash line in Fig. 3 shows Eq.(3) with fitting parameter obtained from enthalpy relaxation experiment. $1/K_Q$ closely follows, $R^2 = 0.79$, the exponential decay function with $\beta = 0.74$ and $\tau_{KWW} = 11{,}000$ s, characteristic of the enthalpy relaxation of the same glass at the same annealing temperature. The quality of the fitting reveals that $K_Q(t)$ follows a similar stretched exponential behavior as $\Delta H_{rel}(t)$ and saturates at $K_{Q,0} = 43.5$ MPa·m$^{1/2}$.

The observation that K_Q follows the stretched exponential decay function as determined by the enthalpy relaxation reveals that the origin of embrittlement is the different structures the system samples at different annealing times (and temperatures). In other words, the origin of embrittlement are the characteristics of the available structural states. As we anneal at a constant temperature, above-mentioned thermal expansion contribution to the free volume (only occurring on the T scale) does not contribute to the annealing-induced embrittlement. Additional evidence that the thermal expansion contribution of the free volume has a negligible effect on K_Q comes from measurements at different temperatures (Fig. 3). K_Q of a relaxed glass ($T_f = 573$ K), measured at $T = 573$ K of 45 ± 3 MPa·m$^{1/2}$ is, within experimental errors, identical to K_Q determined at RT of the same relaxed glass of 43 ± 3 MPa·m$^{1/2}$ (Fig. 3, ◇ and ◇). These glasses exhibit the same structural state and only differ in the second contribution to the free volume, the thermal expansion contribution. Relaxing glasses all the way to their supercooled liquid state is achieved by changing both T_f and T (path 2 in Fig. 3). Specifically, for T_f = 673 K exhibits K_Q = 103.3 ± 3 MPa·m$^{1/2}$, significantly higher than $K_Q = 45 \pm 3$ MPa·m$^{1/2}$ for T_f = 573 K. With the above argument, we can explain this significant change

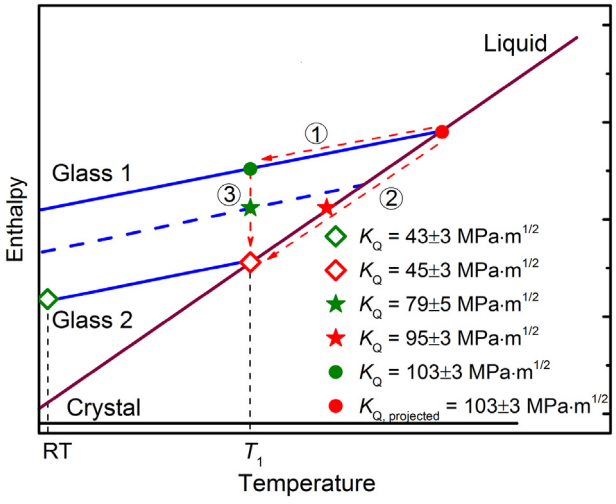

Fig. 3. Enthalpy versus temperature for the supercooled liquid (relaxed glass), various glasses, and the crystalline state. Changes of enthalpy and K_Q as a function of T (path 1), time from a glass towards the metastable equilibrium of the supercooled liquid (path 3), and fictive temperature and temperature while maintaining metastable equilibrium (path 2). Glasses at different temperatures, ◇ and ◇, exhibit identical, within errors, K_Q. In contrast, relaxed glasses with different T_f exhibit widely different K_Q. Glasses processed through path 1&3 and path 2 exhibit the same K_Q indicating that K_Q is a state function.

in K_Q solely by the structural rearrangement contribution to the free volume.

To further reveal the microscopic characteristics of the two contributions to the free volume, we carried out MD simulations (specifics of the MD simulation can be found in the Supplementary material) (Fig. 4). Two different characteristics of particle positions were identified. Cooling from high to low temperature result in glass formation at T_1 (path 1 in Fig. 3), particles move in an affine manner, corresponding to thermal expansion contributions to the free volume. In the case where the system remains in metastable equilibrium (path 2 in Fig. 3), affine movement of all particles still occurs. However, simultaneously, non-affine rearrangement of particles occurs which can be considered as the structural rearrangements of atoms, so-called α-relaxation.

It is important to point out that the overall structural free volume value (measured as enthalpy here) by itself does not unambiguously quantify a glass' fracture toughness when departing in the processing from metastable equilibrium (e.g., path 3 in Fig. 3). For example, ★ and ★ in Fig.3 have the same overall contribution to free volume due to structural rearrangements but differ in K_Q due to the plurality of relaxation processes. The fast processes occur earlier, resulting in a structure that is different from the structure with the same overall contribution to free volume due to structural rearrangements where all relaxation processes (slow and fast) are completed. Only when both paths merge in the supercooled liquid state (◇) the same structure is assumed and hence the same K_Q is observed, revealing the state function nature of K_Q.

Our finding has also technological ramifications. An object made of a MG used in service over time and temperature will embrittle. Such

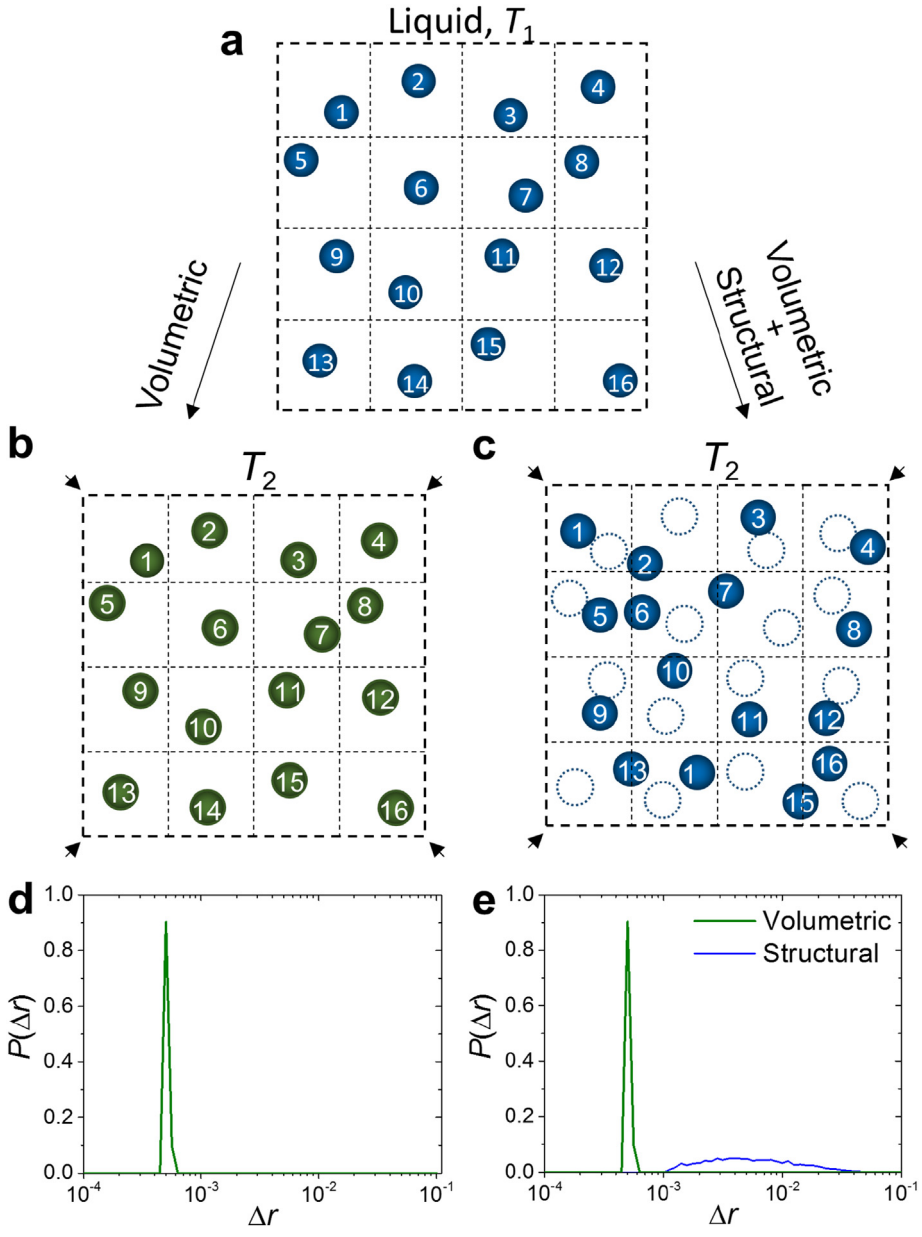

Fig. 4. (a–c) Schematic diagrams to illustrate the thermal expansion and structural rearrangement contribution to the free volume through atomic arrangements in a glass and a liquid at temperatures T_1 and T_2, where $T_1 > T_2$. (a) Possible atomic configuration of liquid at T_1. (b) Quenching the liquid at T_1 into glass at T_2(path 1 in Fig. 3) only results in thermal contraction to the free volume, while (c) remaining in metastable equilibrium from T_1 to T_2 (path 2 in Fig. 3) results in thermal contraction and structural rearrangements (d)–(e) Molecular Dynamics (MD) simulations of distribution of volumetric and structural atomic displacements of binary Lennard-Jones glass during athermal quasistatic compression from 0% strain to 10% strain (in 400 independent glass samples each with N = 2000 atoms). (d) Thermal contraction only results in volumetric changes (narrow peak in P(Δr)). (e) Maintaining in metastable equilibrium from T_1 to T_2 gives rise to two peaks in P(Δr): a narrow peak from the $H_{volumetric}$ contribution and a broad peak from $H_{structural}$.

embrittlement can however not be precisely predicted from enthalpy recovery experiments. For example, $\tau_{average}$ at RT may be very large but within the plurality of relaxation processes, fast relaxation processes will be much further progressed than suggested by the $\tau_{average}$ and the enthalpy recovery. In such cases, glasses can be significantly further embrittled than suggested by their average relaxation time.

In conclusion, embrittlement during annealing of $Zr_{44}Ti_{11}Cu_{10}Ni_{10}Be_{25}$ was determined. The embrittlement kinetics, quantified by K_Q measurements was compared to the kinetics of structural relaxation. Both kinetics follow the same KWW stretched exponential function with the same fitting parameter, β and τ. This reveals that embrittlement in MGs is defined by free volume contribution due to structural rearrangements, whereas free volume due to thermal expansion can be neglected.

Acknowledgement

This work was supported by the Department of Energy through the Office of Basic Energy Sciences (#DE SC0004889).

Appendix A. Supplementary data

Supplementary data to this article can be found online at https://doi.org/10.1016/j.scriptamat.2018.01.024.

References

[1] G. Williams, D.C. Watts, Trans. Faraday Soc. 66 (1970) 80–85.
[2] F. Kohlrausch, Pogg. Ann. Phys. 119 (1863) 352.
[3] R. Bohmer, K.L. Ngai, C.A. Angell, D.J. Plazek, J. Chem. Phys. 99 (1993) 4201–4209.
[4] P.-G. de Gennes, Macromolecules 35 (2002) 3785–3786.
[5] R. Böhmer, K.L. Ngai, C.A. Angell, D.J. Plazek, J. Chem. Phys. 99 (1993) 4201–4209.
[6] J.C. Phillips, Rep. Prog. Phys. 59 (1996) 1133.
[7] O. Lieleg, J. Kayser, G. Brambilla, L. Cipelletti, A.R. Bausch, Nat. Mater. 10 (2011) 236–242.
[8] J.R. Lewandowski, M.E. Halse, M. Blackledge, L. Emsley, Science 348 (2015) 578–581.
[9] J.C. Qiao, J.M. Pelletier, Intermetallics 19 (2011) 9–18.
[10] J.C. Qiao, J.M. Pelletier, Intermetallics 28 (2012) 40–44.
[11] G.J. Fan, J.F. Loffler, R.K. Wunderlich, H.J. Fecht, Acta Mater. 52 (2004) 667–674.
[12] S.G. Mayr, J. Appl. Phys. 97 (2005), 096103.
[13] J.F. Wang, L. Liu, J.Z. Xiao, T. Zhang, B.Y. Wang, C.L. Zhou, W. Long, J. Phys. D. Appl. Phys. 38 (2005) 946.
[14] O. Haruyama, Y. Nakayama, R. Wada, H. Tokunaga, J. Okada, T. Ishikawa, Y. Yokoyama, Acta Mater. 58 (2010) 1829–1836.
[15] O. Haruyama, H. Sakagami, N. Nishiyama, A. Inoue, Mater. Sci. Eng. A 449–451 (2007) 497–500.
[16] R. Busch, E. Bakke, W.L. Johnson, Acta Mater. 46 (1998) 4725–4732.
[17] G. Kumar, D. Rector, R.D. Conner, J. Schroers, Acta Mater. 57 (2009) 3572–3583.
[18] G. Kumar, S. Prades-Rodel, A. Blatter, J. Schroers, Scr. Mater. 65 (2011) 585–587.
[19] A. Castellero, D.I. Uhlenhaut, B. Moser, J.F. Loffler, Philos. Mag. Lett. 87 (2007) 383–392.
[20] D. Deng, A.S. Argon, Acta Metall. 34 (1986) 2011–2023.
[21] T.W. Wu, F. Spaepen, Philosophical Magazine B-Physics of Condensed Matter Statistical Mechanics Electronic Optical and Magnetic Properties 61 (1990) 739–750.
[22] K.J. Laws, D. Granata, J.F. Löffler, Acta Mater. 103 (2016) 735–745.
[23] M. Yan, J.F. Sun, J. Shen, J. Alloys Compd. 381 (2004) 86–90.
[24] H. Kato, T. Ichitsubo, H. Igarashi, A. Inoue, Appl. Phys. Lett. 95 (2009), 231911.
[25] P. Murali, U. Ramamurty, Acta Mater. 53 (2005) 1467–1478.
[26] R. Raghavan, P. Murali, U. Ramamurty, Acta Mater. 57 (2009) 3332–3340.
[27] J.J. Lewandowski, W.H. Wang, A.L. Greer, Philos. Mag. Lett. 85 (2005) 77–87.
[28] C.H. Rycroft, E. Bouchbinder, Phys. Rev. Lett. 109 (2012) 194301.
[29] D. Suh, R.H. Dauskardt, J. Non-Cryst. Solids 317 (2003) 181–186.
[30] A. Slipenyuk, J. Eckert, Scr. Mater. 50 (2004) 39–44.
[31] K.M. Flores, D. Suh, R.H. Dauskardt, P. Asoka-Kumar, P.A. Sterne, R.H. Howell, J. Mater. Res. 17 (2011) 1153–1161.
[32] M.E. Launey, R. Busch, J.J. Kruzic, Acta Mater. 56 (2008) 500–510.
[33] K.S. Lee, J. Eckert, Y.W. Chang, J. Non-Cryst. Solids 353 (2007) 2515–2520.
[34] U. Ramamurty, M.L. Lee, J. Basu, Y. Li, Scr. Mater. 47 (2002) 107–111.
[35] M.E. Launey, R. Busch, J.J. Kruzic, Scr. Mater. 54 (2006) 483–487.
[36] J. Ketkaew, Z. Liu, W. Chen, J. Schroers, Phys. Rev. Lett. 115 (2015) 265502.
[37] A. Inoue, T. Masumoto, H.S. Chen, J. Mater. Sci. 20 (1985) 4057–4068.
[38] T.H. Noh, A. Inoue, H. Fujimori, T. Masumoto, I.K. Kang, J. Non-Cryst. Solids 110 (1989) 190–194.
[39] C.A. Angell, J. Non-Cryst. Solids 131 (1991) 13–31.
[40] O. Haruyama, T. Moftate, K. Morita, N. Yamamoto, H. Kato, T. Egami, Mater. Trans. 55 (2014) 466–472.
[41] R. Raghavan, P. Murali, U. Ramamurty, Metallurgical and Materials Transactions A-Physical Metallurgy and Materials Science 39A (2008) 1573–1577.
[42] J. Xu, U. Ramamurty, E. Ma, Jom-Us 62 (2010) 10–18.
[43] R.L. Narayan, P. Tandaiya, G.R. Garrett, M.D. Demetriou, U. Ramamurty, Scr. Mater. 102 (2015) 75–78.
[44] W. Chen, J. Ketkaew, Z. Liu, R.M.O. Mota, K. O'Brien, C.S. da Silva, J. Schroers, Scr. Mater. 107 (2015) 1–4.
[45] W. Chen, H. Zhou, Z. Liu, J. Ketkaew, L. Shao, N. Li, P. Gong, W. Samela, H. Gao, J. Schroers, Acta Mater. 145 (2018) 477–487.
[46] J. Ketkaew, Z. Liu, W. Chen, J. Schroers, Phys. Rev. Lett. 115 (2015).
[47] W. Chen, Z. Liu, J. Ketkaew, R.M.O. Mota, S.H. Kim, M. Power, W. Samela, J. Schroers, Acta Mater. 107 (2016) 220–228.
[48] H.Z.W. Chen, Z. Liu, J. Ketkaew, N. Li, J. Yurko, N. Hutchinson, H. Gao, J. Schroers, Scr. Mater. 130 (2017) 152–156.
[49] B. Sarac, J. Schroers, Nat. Commun. 4 (2013).
[50] J. Ketkaew, H. Wang, W. Chen, G. Pereira, Z. Liu, W. Dmowski, E. Bouchbinder, C.S. O'Hern, T. Egami, J. Schroers, Nature Communicationssubmitted 2017.
[51] I.R. Lu, G.P. Görler, H.J. Fecht, R. Willnecker, J. Non-Cryst. Solids 274 (2000) 294–300.
[52] L. Shadowspeaker, R. Busch, Appl. Phys. Lett. 85 (2004) 2508–2510.
[53] B. Sarac, J. Ketkaew, D.O. Popnoe, J. Schroers, Honeycomb structures of bulk metallic glasses, Adv. Funct. Mater. 22 (2012) 3161–3169.
[54] W. Gotze, L. Sjogren, Rep. Prog. Phys. 55 (1992) 241.
[55] T.A. Vilgis, Phys. Rev. B 47 (1993) 2882–2885.
[56] I. Gallino, M.B. Shah, R. Busch, Acta Mater. 55 (2007) 1367–1376.
[57] C. Nagel, K. Rätzke, E. Schmidtke, J. Wolff, U. Geyer, F. Faupel, Phys. Rev. B 57 (1998) 10224–10227.
[58] J.N. Mei, J.L. Soubeyroux, J.J. Blandin, J.S. Li, H.C. Kou, H.Z. Fu, L. Zhou, J. Non-Cryst. Solids 357 (2011) 110–115.
[59] Z. Evenson, R. Busch, Acta Mater. 59 (2011) 4404–4415.